



**HAL**  
open science

# Ionic Liquid Driven Enhancement in the Electromagnetic Interference Shielding Effectiveness of Poly(methyl-methacrylate)-Based Composite Materials Filled with Hybrid Silver-Coated Glass Microfibers

Clémence Retailleau, Jalal Alaa-Eddine, Fabien Ndagijimana, Pierre Alcouffe, Laurent Cavetier, Matthieu Fumagalli, Véronique Bounor-Legaré, Anatoli Serghei

## ► To cite this version:

Clémence Retailleau, Jalal Alaa-Eddine, Fabien Ndagijimana, Pierre Alcouffe, Laurent Cavetier, et al.. Ionic Liquid Driven Enhancement in the Electromagnetic Interference Shielding Effectiveness of Poly(methyl-methacrylate)-Based Composite Materials Filled with Hybrid Silver-Coated Glass Microfibers. *Macromolecular Materials and Engineering*, 2022, 307 (3), pp.2100759. 10.1002/mame.202100759 . hal-03853897

**HAL Id: hal-03853897**

**<https://hal.science/hal-03853897>**

Submitted on 15 Nov 2022

**HAL** is a multi-disciplinary open access archive for the deposit and dissemination of scientific research documents, whether they are published or not. The documents may come from teaching and research institutions in France or abroad, or from public or private research centers.

L'archive ouverte pluridisciplinaire **HAL**, est destinée au dépôt et à la diffusion de documents scientifiques de niveau recherche, publiés ou non, émanant des établissements d'enseignement et de recherche français ou étrangers, des laboratoires publics ou privés.

**Ionic liquid driven enhancement in the electromagnetic interference shielding effectiveness of poly(methyl-methacrylate) based composite materials filled with hybrid silver-coated glass microfibers**

Clémence RETAILLEAU<sup>1</sup>, Jalal ALAA-EDDINE<sup>2</sup>, Fabien NDAGIJIMANA<sup>2</sup>,  
Pierre ALCOUFFE<sup>1</sup>, Laurent CAVETIER<sup>1</sup>, Matthieu FUMAGALLI<sup>1</sup>,  
Véronique BOUNOR-LEGARE<sup>1</sup>, Anatoli SERGHEI<sup>1\*</sup>

<sup>1</sup>*Université Claude Bernard Lyon, Ingénierie des Matériaux Polymères, Lyon, France*

<sup>2</sup>*Université de Grenoble Alpes, Grenoble, France*

**Keywords:** electromagnetic interference shielding; conductive polymer composites; ionic liquids; hybrid fillers; microfibers;

**Abstract**

The electromagnetic interface shielding properties of poly(methyl-methacrylate) based composite materials filled with hybrid silver-coated glass microfibers are investigated between 100 kHz and 1 GHz using the coaxial cell method. The incorporation of the ionic liquid EMPy-TFSI (1-ethyl-4-methylpyridinium bis(trifluoromethylsulfonyl)) into the composite material leads to a substantial decrease in the percolation threshold and to an enhancement in the electromagnetic interference shielding effectiveness by more than 60 dB. The addition of EMPy-TFSI, selected for its excellent compatibility with the polymer matrix, allows one to obtain composite materials with shielding effectiveness values up to 116 dB, as compared to a maximum value of 43 dB obtained in the absence of the ionic liquid. This enhancement effect is explained by the interactions between the ionic liquid, the polymer matrix and the silver-coated microfibers that lead to a more efficient percolation network. The use of ionic liquids could represent thus a powerful approach to develop functional composite materials with enhanced interference shielding properties.

**\*Corresponding author:** anatoli.serghei@univ-lyon.fr

## 1. Introduction

Developing materials with enhanced performance in shielding electromagnetic interference phenomena is increasingly becoming a major challenge in our society, driven by the ubiquitous presence of electromagnetic pollution. Polymer-based conductive composites represent efficient materials to shield the undesired impact of the electromagnetic pollution on the secure functioning of systems and devices. They offer in the same an excellent alternative to metallic electromagnetic shields. The latter show superior shielding properties but present numerous drawbacks related to processing, costs, weight and flexibility [1,2]. Polymer materials, electrically insulating by their nature, can be used as host matrices for developing conductive composite materials by adding conductive fillers of different sizes (micrometric or nanometric), nature (metallic or carbon based) and aspect ratio (spherical, nanowires/nanotubes, etc.) [3–9]. Above a certain filler concentration (called the percolation threshold), the composite materials become conductive due to the formation of a long range percolation network through the local electrical contacts between the fillers and tunneling effects [3,10–12]. As shown in numerous studies in the scientific literature [2,13–15], the electromagnetic shielding effectiveness is tightly correlated to the material conductivity, through three distinct shielding mechanisms: simple reflection, absorption and multiple reflections. Additionally, in the case of magnetic composites, the magnetic permeability plays also an important role, too [13,16]. Three key-parameters play the most important role in determining the conductivity of composite materials: the intrinsic conductivity of the fillers (determined by their nature), the quality of the filler/filler local electrical contacts (mediated by the molecular interactions with the polymer matrix) and the number density of the filler/filler electrical contacts in the volume of the composite material (determined by the size, aspect ratio and volume concentration of fillers). For a given polymer matrix and for fillers with a given intrinsic conductivity, size and aspect ratio, increasing the conductivity of a composite material (and consequently its shielding effectiveness) relies essentially on increasing the volume concentration of fillers [1,3,4]. This, however, usually creates important difficulties related to material processing, mechanical properties, weight and costs. Finding new alternative approaches for enhancing the shielding properties of composite materials without increasing the amount of fillers represent therefore an important challenge. In the scientific literature, this challenge has been addressed in several different ways. Most obviously, a first approach consists in optimizing the processing method used for the preparation of the composite materials. Different processing methods, such as melt-mixing (by internal mixer or extrusion),

injection moulding, solvent casting, are known to lead to significant differences in the shielding properties of composite materials [17–19] due to changes in the local distribution and dispersion of fillers. Another possible approach of increasing the shielding effectiveness without increasing the amount of fillers has been addressed by developing microporous polymer foams [20–24]. The foam porosity created by the presence of the air cavities leads, by exclusion effects, to a local increase in the filler effective concentration in the polymer matrix, giving rise to a higher shielding effectiveness. A further approach consists in using blends of immiscible polymers with two or more polymer phases [25–29], leading to a percolation phenomenon that selectively occurs in the more compatible polymer phase. Other alternative approaches of enhancing the shielding performance of composite materials by functionalizing the surface of the fillers [30–33] or by adding lubricants or thermal stabilizers [19] have been reported, as well.

In the present study it is shown that the electromagnetic shielding properties of a polymer-based composite material filled with hybrid silver-coated microfibers can be greatly enhanced by the impact of an ionic liquid. In the same time, a much lower percolation threshold is obtained, as well. In the presence of the ionic liquid, polymer-based composite materials reaching shielding effectiveness values as high as 116 dB are obtained, much higher than those obtained in the absence of the ionic liquid (43 dB). Ionic liquids can represent thus very efficient means to develop polymer based composite materials with enhanced electromagnetic shielding properties.

## **2. Experimental**

### **2.1 Materials**

Two different poly(methyl methacrylate) matrices have been used in our study: Altuglas V825T (PMMA\_A, supplied by Arkema, melt flow index of 2.8 g/10 min, density of 1.18 g/cm<sup>3</sup>, Vicat softening temperature of 112°C) and Altuglas VSUVT (PMMA\_B, supplied by Arkema, melt flow index of 28 g/10 min, density of 1.18 g/cm<sup>3</sup>, Vicat softening temperature of 93°C). Silver-coated glass microfibers (AgGF, SF82TF20) purchased from Hart Material Ltd (UK) were used as fillers. The fillers have a density of 2.8 g/cm<sup>3</sup>, an average length of 100 µm and an average diameter of 17 µm. The ionic liquid (IL) used in our study was EMPy-TFSI (1-ethyl-4-methylpyridinium bis(trifluoromethylsulfonyl)imide), supplied by Iolitech (density of 1.49 g/cm<sup>3</sup>, bulk conductivity of 3.42 mS/cm).

## 2.2 Composite preparation

A schematic representation of the experimental procedure used to prepare our composite materials is given in Fig. 1. Composite materials with different filler concentrations have been prepared by melt blending at 210°C using a Haake PolyLab internal mixer (Haake™ Rheomix). The internal mixer had two counter rotating roller rotors and a total mixing volume of 50 cm<sup>3</sup>. The rotors speed was fixed to 80 rpm. The composite preparation took place in three steps. PMMA was introduced first and mixed until torque stabilization. The ionic liquid EMPy-TFSI was subsequently added into the PMMA matrix and mixed until torque stabilization. Finally, the fillers AgGF were added into the PMMA/IL blend until torque stabilization followed by additional 10 min of mixing. During the mixing period, temperature and torque were continuously recorded. Subsequently, each formulation was cooled down to ambient temperature. Discs with a thickness of 1 mm and a diameter of 21 mm were then prepared by compression moulding at 210 °C using a laboratory press Polysat 200T. The compositions of the composite materials investigated in our study are summarized in Table 1.

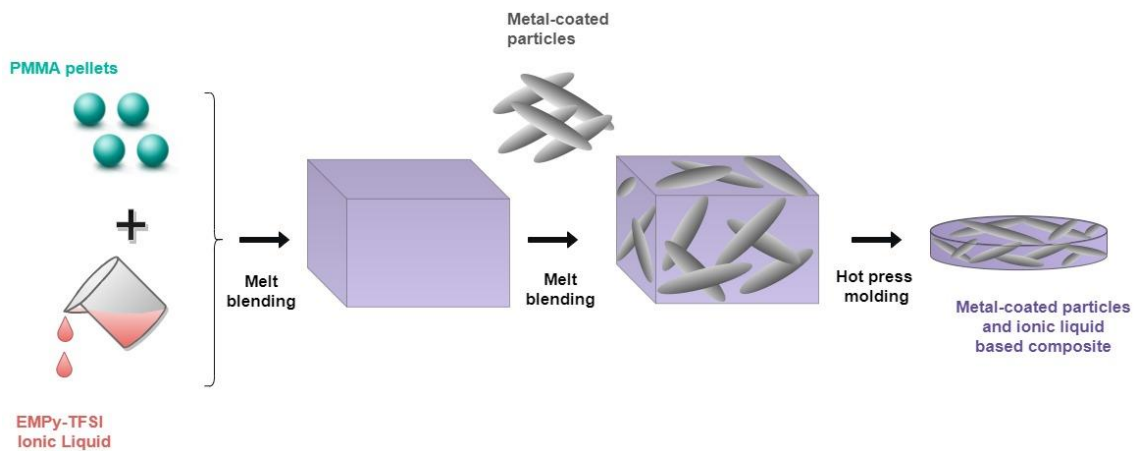


**Figure 1:** Schematic representation of the experimental procedure used to prepare PMMA/AgGF/IL composite materials.

**Table 1:** Composition of the investigated composite materials

Name	AgGF (vol%)	IL (vol%)	Name	AgGF (vol%)	IL (vol%)
PMMA (Altuglas® V825T)			PMMA (Altuglas® V825T)		
PMMA_A_5_AgGF	5	0	PMMA_A_20_AgGF_5_IL	20	5
PMMA_A_10_AgGF	10	0	PMMA_A_20_AgGF_10_IL	20	10
PMMA_A_15_AgGF	15	0	PMMA_A_20_AgGF_40_IL	20	40
PMMA_A_20_AgGF	20	0	PMMA_A_10_AgGF_10_IL	10	10
PMMA_A_30_AgGF	30	0	PMMA_5_IL	0	5
PMMA_A_5_AgGF_20_IL	5	20	PMMA_10_IL	0	10
PMMA_A_10_AgGF_20_IL	10	20	PMMA_20_IL	0	20
PMMA_A_15_AgGF_20_IL	15	20	PMMA_40_IL	0	40
PMMA_A_20_AgGF_20_IL	20	20	PMMA (Altuglas® VSUVT)		
PMMA_A_30_AgGF_20_IL	30	20	PMMA_B_10_AgGF	10	0

## 2.3 Sample Characterization

### EMI shielding test

The coaxial cell method corresponding to the ASTM-4935 standard was employed to measure the EMI shielding properties of our composite materials in the frequency range from 100 kHz to 1 GHz (Fig. 2), using an Anritsu Vector Network Analyzer (Stockline MS46522B-20). A TOSLKF50A-20 Type K(f) calibration kit was used to calibrate the measurement cell. Each sample, in form of an annular shape with an outer diameter of 21 mm, inner diameter of 6 mm and thickness of 1 mm, has been measured at least three times. The contact zones of the samples with the coaxial measurement cell have been gold-metallized by sputtering in order to completely eliminate the impact of the contact resistance on the shielding measurement (Fig. 2 b).

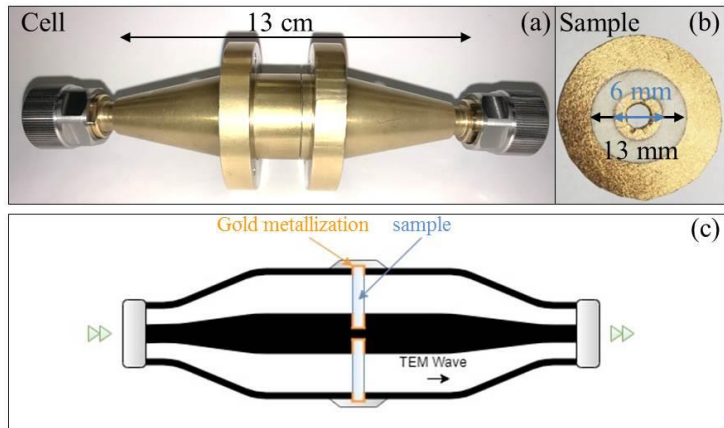


**Figure 2:** (a) coaxial measurement cell used in our study; (b) sample configuration in a coaxial measurement cell; (c) schematic representation of the coaxial measurement cell.

### Conductivity measurements

The conductivity measurements have been carried-out from 1 MHz to 1 Hz using a High-Resolution Dielectric Spectrometer (Alpha-Analyser) from Novocontrol GmbH. The electrical investigations have been performed by employing a 2-electrode geometry on the same samples used for the EMI shielding test. Thus, the same direction of the electric field has been investigated in both experiments. The contribution of the contact resistance has been eliminated by gold-metallizing the contact zones between the samples and the measurement electrodes. The applied electric voltage was 0.1 V and the measurements have been carried-out at ambient temperature.

### Differential Scanning Calorimetry (DSC)

DSC analysis was performed on sample amounts of 3–5 mg using a TA Instruments Q200 apparatus operating under ambient atmosphere. The DSC instrument was calibrated using indium standards. Two heating/cooling ramps were performed at a scanning rate of 10 C/min from  $-40\text{ }^{\circ}\text{C}$  to  $250\text{ }^{\circ}\text{C}$ . The glass transition temperature was taken as the average value calculated from experimental data obtained on three different samples for each composite material.

## Rheology

The rheological measurements were carried-out in dynamic mode using a Discovery Hybrid Rheometer DHR (TA instruments). All measurements were performed at 160°C under ambient atmosphere, using a parallel plate geometry (diameter = 25 mm). The linear viscoelastic deformation limit was carefully determined for each sample. Frequency sweep experiments were performed from 100 rad.s<sup>-1</sup> to 0.01 rad.s<sup>-1</sup>, by applying a constant stress of 100 Pa in order to stay in the linear viscoelastic regime.

## Microscopy

The filler dispersion was characterized by optical microscopy using an OLYMPUS BX41 microscope. Prior to observation, the samples were cut into 20 µm thick sections parallel to the discs surface. To determine the average size of the microfibers, the fillers were extracted by dissolving the PMMA matrix in acetone under sonication. The average size of the fillers was then determined using the image processing software Image J. Scanning electron microscope (SEM) analysis was carried out on polished samples to investigate the silver coating of the glass microfibers within the PMMA matrix. The extracted fillers were also analysed by SEM using a Hitachi S800 apparatus, by applying an acceleration voltage of 5 kV and employing a backscattering detector.

## 3. Results and discussion

The electromagnetic interference shielding effectiveness (EMI SE) of a given shield is given by:

$$EMI\ SE[dB] = 10 \log \left| \frac{P_i}{P_t} \right| = 20 \log \left| \frac{H_i}{H_t} \right| = 20 \log \left| \frac{E_i}{E_t} \right| \quad (1)$$

where  $P_i$ ,  $E_i$  and  $H_i$  are the power, electric field amplitude and magnetic field amplitude of the incident electromagnetic wave, and  $P_t$ ,  $E_t$  and  $H_t$  the power, electric field amplitude and magnetic field amplitude of the electromagnetic wave transmitted through the shield. A shielding effectiveness of 40 dB, for instance, corresponds to 0.01 % of the incident electromagnetic power that gets transmitted through the electromagnetic shield. When an

incident electromagnetic wave falls onto a shielding material (Fig. 3), several phenomena take place, governed by the interaction EM wave/matter. First, a part of the EM wave gets reflected at the rear air/material interface and does not penetrate into the shielding material at all. This phenomenon, called simple reflection, is due to the discontinuity in the wave impedance at the first air/material interface:

$$\mathbf{Z} = \frac{\mathbf{E}}{\mathbf{H}} = \sqrt{\frac{\mu^*}{\epsilon^*}} = \sqrt{\frac{j\omega\mu'}{\sigma + j\omega\epsilon'}} \quad (2)$$

where E and H are the electric and magnetic field of the EM wave in the material, respectively,  $\omega$  the angular frequency ( $\omega = 2\pi f$ , with f the wave frequency),  $\mu'$  and  $\epsilon'$  the real part of the permeability and permittivity, respectively,  $\sigma$  is the electrical conductivity of the material and j the imaginary number  $\sqrt{-1}$ . The other part of the EM wave penetrates into the material and gets partially absorbed all along the way through the electromagnetic shield. This shielding mechanism, called absorption, is governed by a characteristic parameter related to the skin-depth of the material, defined as:

$$\delta = \sqrt{\frac{2}{\mu'\omega\sigma}} = \sqrt{\frac{1}{\mu'\pi f\sigma}} \quad (3)$$

The skin-depth decreases with increasing conductivity, frequency and magnetic permeability. The smaller the skin-depth is, the higher gets the electromagnetic absorption. The part of the electromagnetic wave arriving at the back interface of the shielding material is reflected once again and travels back to the rear-interface where is reflected again and so on, getting gradually absorbed at every passage between the two air/material interfaces. This shielding mechanism is called multiple reflections.

Consequently, three major mechanisms contribute to the shielding properties of materials: simple reflexion, absorption and multiple reflexions. They can be expressed as:

$$\mathbf{SE}_T = \mathbf{SE}_A + \mathbf{SE}_R + \mathbf{SE}_M \quad (4)$$

with

$$SE_A = 20 \cdot \frac{d}{\delta} \log_{10}(e) \quad (5)$$

$$SE_R = -20 \cdot \log_{10} \left( \left| \frac{4Z_0 Z}{(Z+Z_0)^2} \right| \right) \quad (6)$$

$$SE_M = 20 \cdot \log_{10} \left( \left| 1 - \left( \frac{Z-Z_0}{Z+Z_0} e^{-d/\delta} \right)^2 \right| \right) \quad (7)$$

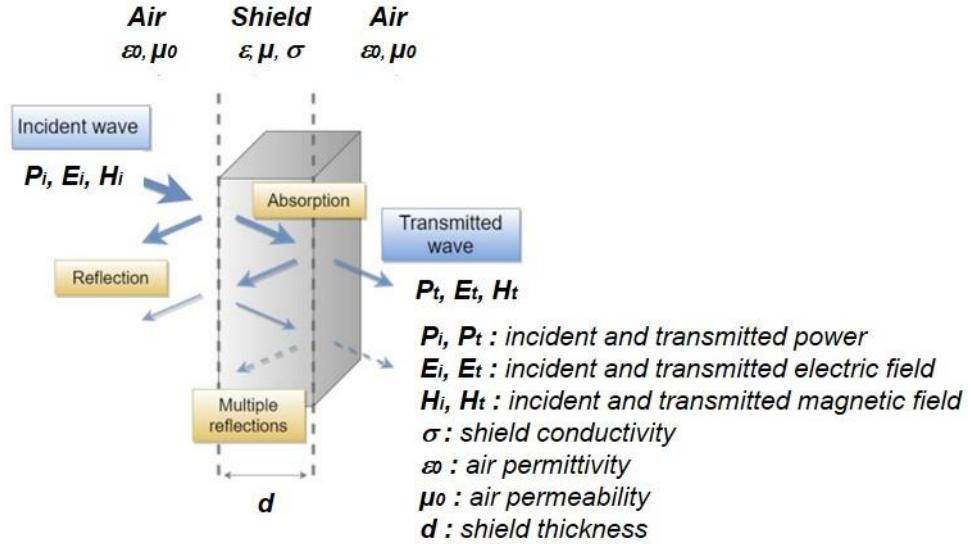


**Figure 3:** Schematic representation of the EMI shielding mechanisms.

The electrical properties of PMMA\_A/AgGF composite materials at different filler concentrations are presented in Fig. 4a, as a function of frequency. The conductivity spectra indicate a dielectric behaviour for 0 vol%, 5 vol% and 10 vol% AgGF, corresponding to negligible conductivity values. Starting from 15 vol% AgGF, the composite begins to show significant conductive properties manifested as a frequency independent plateau related to the conductivity value of the investigate material. The conductivity rapidly increases with the filler content, reaching 1.93 S/cm at 20 vol% AgGF and 9.20 S/cm at 30 vol% AgGF.

The electromagnetic shielding spectra of PMMA\_A/AgGF composite materials at different filler concentrations are presented in Fig. 4b, in the frequency range from  $10^5$  Hz to  $10^9$  Hz. While the composites with filler concentrations of 5 vol%, 10 vol% and 15 vol% exhibit negligible electromagnetic interference shielding effectiveness (EMISE) values, significant shielding properties are obtained with 20 vol% and 30 vol%. In the low frequency range, the EMISE spectra show a constant plateau behaviour, related to the conductivity value of the composite materials. The main shielding contribution in this frequency region is governed by

the mechanism of simple reflexion. At higher frequencies, a slight increase in the EMISE values is observed, indicating the onset of absorption effects.

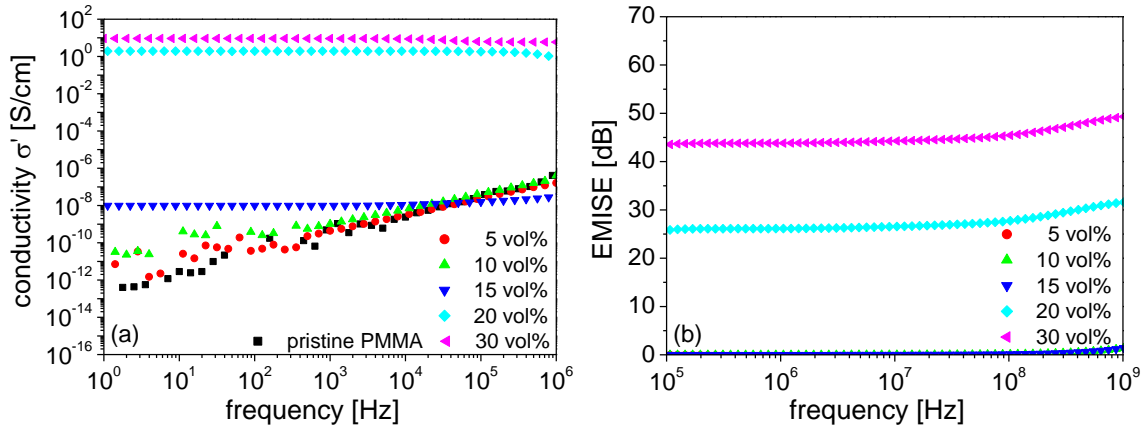


**Figure 4:** conductivity spectra (a) and electromagnetic shielding spectra (b) of PMMA\_A/AgGF composite materials, as a function of frequency, for different filler concentrations of AgGF, as indicated.

Adding the ionic liquid (1-ethyl-4-methylpyridinium bis-trifluoromethylsulfonyl) (EMPy-TFSI) into the PMMA\_A/AgGF composite material leads to a substantial increase in the shielding effectiveness. This is shown in Fig. 5, where EMISE spectra of PMMA\_A/AgGF/EMPy-TFSI materials are presented at different AgGF filler concentrations and 20 vol% of EMPy-TFSI. Much higher EMISE values are obtained, reaching a maximum shielding effectiveness of 117 dB, while a maximum of 43 dB is reached in the absence of the ionic liquid. A much earlier onset of absorption effects is observed as well, leading to rapidly increasing shielding properties at high frequencies. After passing through a maximum value, the shielding effectiveness begins to decrease. This is due to inductive effects characteristic for the metallic conductivity that lead to an increase in the sample impedance at high frequencies and give rise to a decrease in the shielding effectiveness.

The dependence of the EMISE values on the filler concentration at 0 vol% and 20 vol% EMPy-TFSI is shown in Fig. 6, for two different frequencies (100 kHz and 100 MHz). A lower percolation threshold and much higher EMISE values are observed when the ionic liquid is added into the composite material. For instance, at 15 vol% AgGF no shielding is detected for the PMMA\_A/AgGF composite material at 100 MHz, while a shielding of 76 dB is obtained when adding 20 vol% EMPy-TFSI. The enhancement effect takes place in the whole range of

filler concentrations and becomes much larger at higher frequencies (100 MHz) than at lower frequencies (100 kHz) due to the onset of absorption phenomena.

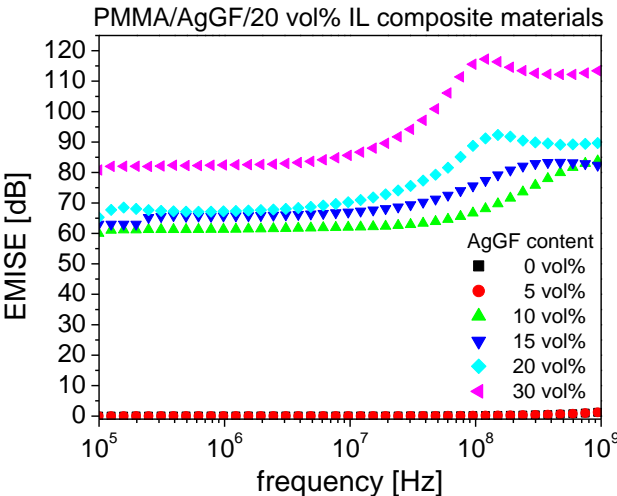


**Figure 5:** EMISE spectra of PMMA\_A/AgGF/20 vol% EMPy-TFSI composite materials as a function of frequency, for different AgGF concentrations, as indicated.

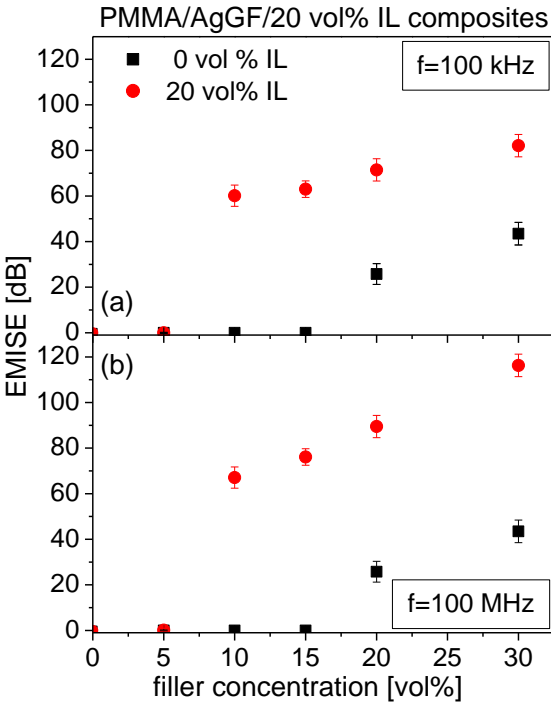


**Figure 6:** EMISE values of PMMA\_A/AgGF/EMPy-TFSI composite materials as a function of filler concentration, without and with the addition of 20 vol% EMPy-TFSI, at two different frequencies: (a) 100 kHz and (b) 100 MHz.

The influence of the concentration of the ionic liquid onto the shielding properties of PMMA\_A/AgGF composite materials has been investigated, as well. The results are presented in Fig. 7, showing the EMISE values obtained at different IL concentrations varying from 0 vol% to 40 vol%, while the AgGF filler concentration was fixed to 20 vol%. A shielding value of 27 dB is obtained at 0 vol% EMPy-TFSI, corresponding to the EMISE spectra presented in Fig. 4b. An enhancement effect of the shielding effectiveness is already observed at 5 vol% IL concentration. When further increasing the IL concentration up to 20 vol%, the shielding effectiveness increases up to 65 dB. For IL concentrations higher than 20 vol%, a saturation plateau is obtained and no further changes in the shielding performance are observed. The optimal EMPy-TFSI concentration appears thus to be 20 vol%.

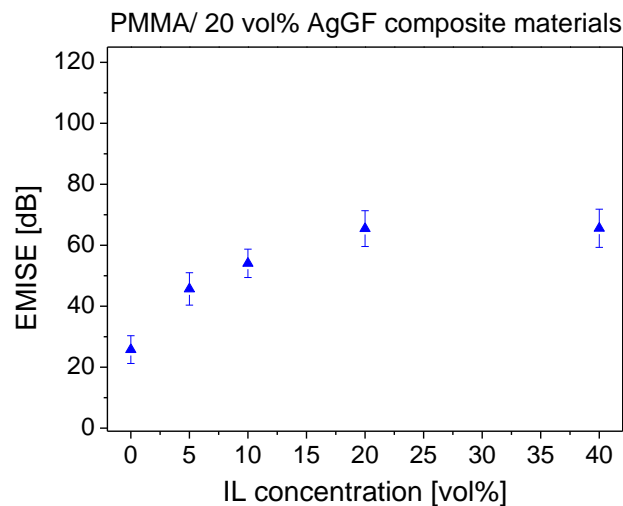


**Figure 7:** EMISE values of PMMA\_A/20vol%AgGF/EMPy-TFSI composite materials as a function of the EMPy-TFSI concentration.

In conclusion, the addition of the ionic liquid turns out to be an effective approach for increasing the shielding properties of composite materials without increasing (or even with decreasing) the amount of fillers. The enhancement effect obtained with the ionic liquid is compared in the following to other approaches reported in the scientific literature. One alternative approach found in the scientific literature consists in using porous foam materials. These materials are employed to obtain a local increase in the effective filler concentration due to exclusion effects induced by the presence of air cavities. For instance, Thomassin et al. [20] studied polycaprolactone(PCL)/carbon nanotubes (MWCNT) composite materials and have shown that foaming at 0.25 vol% MWCNT provides a shielding effectiveness by 40 dB higher

than the un-foamed composite at 0.49 vol% MWCNT. Ameli et al [23] have studied polypropylene(PP)/carbon fibers(CF) composite materials and have shown that, at a constant CF filler concentration of 7.5 vol%, foaming increases the shielding effectiveness from 12 dB to 25 dB. Similar effects were reported by Zhang et al [34] in a study on phenol formaldehyde (PF) resins filled with CF fillers where an increase in the shielding effectiveness by 9 dB is reported due to foaming.

A second alternative approach reported in the scientific literature to enhance the shielding effectiveness of composite materials without increasing the amount of fillers consists in using immiscible polymer blends. These materials are used to obtain a guided electrical percolation by selective molecular interactions taking place in a phase-separated morphology. This is leading to a higher effective local concentration of fillers giving rise to an increase in the shielding effectiveness. For instance, Dou et al. [26] studied polystyrene(PS)/polyvinylidene fluoride(PVDF) blends filled with MWCNT and reported an increase in the shielding effectiveness by 5 dB as compared to the reference composite (PS/MWCNT). Furthermore, by adding a third polymer matrix (high density polyethylene (HDPE)) to the PS/PVDF/1.6 vol% MWCNT blend the shielding effectiveness increased by 13 dB. Rohini and al. [35] showed that PMMA/ PS (50/50 wt%) blends filled with 1 wt% of MWCNT shown an increase by 9 dB in the shielding effectiveness, as compared to the PMMA/1wt%MWCNT composite material.

A third alternative approach found in the scientific literature to increase the shielding effectiveness without increasing the amount of filler consists in functionalizing the filler surface. For instance, Soares et al. [30,31] investigated MWCNT/PS and MWCNT/PP/PLA composite materials and showed that shielding effectiveness increases by 5 dB when the surface of the fillers is functionalized by the use of an ionic liquid. In another study [37], Wu et al. used maleic acid and maleic anhydride to functionalize the MWCNT surface and reported an increase in the shielding effectiveness of MWCNT/(poly(urea urethane)(PUU) composite materials by 7 dB. Im et al. [39] used MWCNT fillers functionalized by flourization and reported a shielding effectiveness of epoxy-based composite materials of 30 dB at 2.25 vol% filler concentration, as compared to 15 dB obtained with the untreated MWCNT.

The different approaches to enhance the shielding effectiveness of composite materials at a constant filler concentration discussed so far are summarized in Table 2 and compared to the experimental results presented in our study. It turns out that the addition of an ionic liquid into the composite material appears to be one of the most effective approaches, leading to an enhancement in the shielding effectiveness by up to 80 dB.

**Table 2 :** Different approaches to enhance the shielding performance of composite materials, compared to the approach presented in the current study.

Nature of filler	Matrix	Approach	Thickness (mm)	Loading amount of fillers	Delta EMI SE		SE [dB]	Ref
					Freq [Hz]	Delta SE [dB]		
MWCNT	PCL	Foams	2	0.25 vol%	$25 \times 10^9$	+ 40	60	[20]
CF	PP	Foams	-	7.5 vol%	$8 \times 10^9$	+ 13	25	[23]
MWCNT	FKM	Foams	3.8	8 wt%	$8 \times 10^9$	+ 4	26	[21]
FGS	PS	Foams	2.5	30 wt%	$8 \times 10^9$	+ 10	30	[22]
SSF	PP	Foams	3.2	1.5 vol%	$8 \times 10^9$	+ 9	49	[36]
CF	PF	Foams	3	2 vol%	$7 \times 10^8$	+ 9	25	[34]
AgGF	PMMA	Add IL	1	10 vol%	$1 \times 10^8$	+ 65	65	This work
AgGF	PMMA	Add IL	2	30 vol%	$1 \times 10^8$	+ 80	116	This work
MWCNT	PS	Funct	1	1 vol%	$8 \times 10^9$	+ 5	8	[30]
MWCNT	PP/PLA	Funct	2	5 wt%	$8 \times 10^9$	+ 5	13	[31]
MWCNT	PUU	Funct	0.7	5 phr	$25 \times 10^9$	+ 7	22	[37]
MWCNT	PP	Funct	-	2 wt%	$20 \times 10^9$	+ 9	16	[38]
MWCNT	Epoxy	Funct	1	1 wt%	$2 \times 10^9$	+ 15	30	[39]
SWCNT	Epoxy	Funct	2	2.25 vol%	$8 \times 10^9$	+ 8	15	[40]
MWCNT	PS/PVD F/HDPE	Blend	-	1.6 vol%	$8 \times 10^9$	+ 13	30	[26]
CB	PP/PS	Blend	2	10 vol%	$1 \times 10^9$	+ 7	20	[41]
CB	PS/EVA	Blend	1	5 wt%	$8 \times 10^9$	+ 5	25	[42]
NH2-MWCNT	PS/PM MA	Blend	1	1wt%	$8 \times 10^9$	+ 9	26	[35]

The impact of the addition of the EMPy-TFSI ionic liquid onto the rheological properties of the PMMA matrix and its glass transition temperature has been investigated in the

current study by Rheology and Differential Scanning Calorimetry (data presented in the Supplementary Information Part). The DSC investigations have revealed a plasticizing effect produced by the presence of the ionic liquid and leading to a decrease in the glass transition temperature of PMMA with increasing the IL concentration. In the same time, in the whole range of IL concentrations studied in the present work (from 5 vol% to 40 vol%), the crystallization process specific to the EMPy-TFSI ionic liquid in the bulk (detected at a temperature of 6 °C) is completely disappearing in the PMMA blend. This indicates a homogenous mixing of the PMMA/EMPy-TFSI blends without any phase separation. At reasonable EMPy-TFSI concentrations (in the range from 5 vol% to 20 vol%), the obtained glass transition of the PMMA/EMPy-TFSI blends remains much higher than the ambient temperature.

The rheological investigations reveal a decrease in the complex viscosity with increasing the concentration of the ionic liquid, due to plasticizing effects (data shown in the Supplementary Information Part). As predicted theoretically, this decrease exhibits a linear dependency in relation to the volume of the ionic liquid (Supplementary Information Part), proving once again the excellent miscibility properties of the ionic liquid with the PMMA polymer matrix. A second PMMA matrix (PMMA\_B), much less viscous than the PMMA polymer discussed so far (PMMA\_A), was investigated as well, with the propose of unravelling the role of viscosity in the enhancement effect on the shielding effectiveness obtained by addition of the ionic liquid. PMMA\_B shows a viscosity lower than the blend PMMA\_A / 10 vol% EMPy-TFSI. In the same time, the composite material PMMA\_B / 10%AgGF and PMMA\_A / 10%AgGF show negligible shielding properties, as opposed to the composite material PMMA\_A / 10 vol% AgGF / 10 vol% EMPy-TFSI which exhibits significant EMISE values (Supplementary Information Part). Considering that PMMA\_B is less viscous than the blend of PMMA\_A with 10 vol% EMPy-TFSI, these results indicate that the viscosity is not the predominant parameter leading to the enhancement effect of the ionic liquid on the shielding properties of the PMMA/AgGF composite materials.

A change in viscosity largely impacts the shear forces experienced by the AgGF microfibers during the melt mixing process. At higher viscosities, the effect of these forces may fracture the microfibers, leading to a decrease in their average length. In this case, a significant impact on the conductive properties (and consequently on the shielding performance) would be expected, since shorter fibers would shift the percolation threshold to higher filler concentrations. In order to exclude this effect, a statistical analysis of the length distribution of

the microfibers has been carried-out (Fig. 8 and Table 3). The analysed fillers were extracted from composite materials prepared with and without the addition of the ionic liquid.

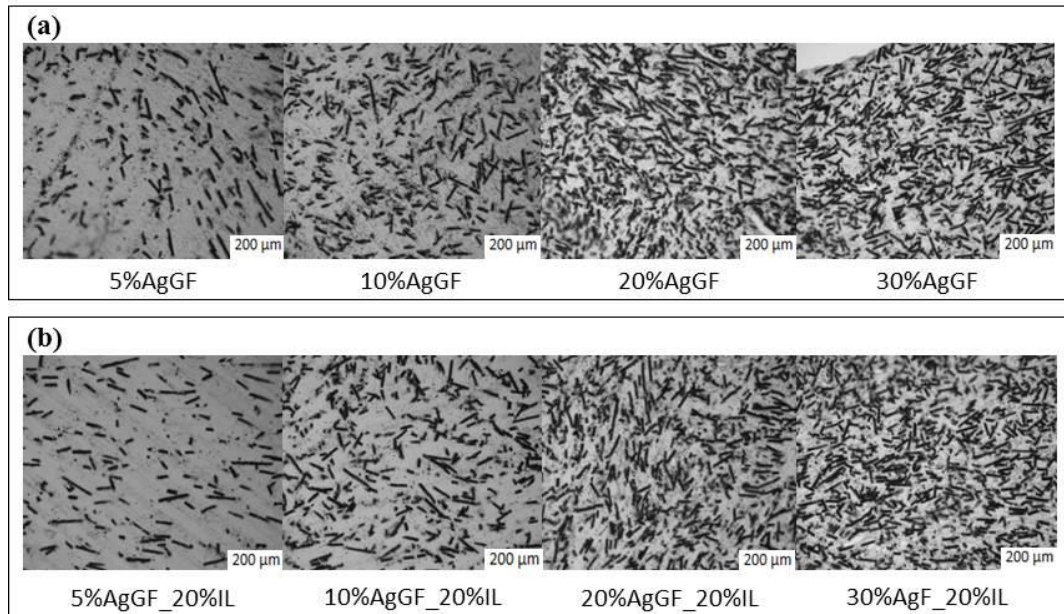


**Figure 8:** Optical images of the AgGF fillers extracted from PMMA/AgGF composite materials prepared using different filler concentrations: (a) without the addition of the ionic liquid; (b) with the addition of 20% vol. EMPy-TFSI.

The fillers have been extracted by dissolving the PMMA into a compatible solvent (acetone), after the preparation process by melt mixing. A quantitative statistical analysis of the length and diameter of fillers was carried-out using the image processing software ImageJ. The results, summarized in Table 3, indicate no significant changes in length and diameter of fillers extracted from the composite materials after melt-mixing. Thus, the composite processing by melt mixing does not seem to affect the size distribution of the silver-coated glass microfibers.

**Table 3:** statistical analysis of the length and diameter of fillers, in dependence on the AgGF filler concentration, without and with the addition of the ionic liquid.

AgGF content (vol%)	Average Length ( $\mu\text{m}$ )	Standard Deviation ( $\mu\text{m}$ )	Average Width ( $\mu\text{m}$ )	Standard deviation ( $\mu\text{m}$ )
Pristine AgGF	109	60	18	2
Without IL				
10	97	53	18	2
20	99	54	18	3
30	105	63	17	3
With IL				
10	107	53	18	3
20	111	58	18	2
30	95	55	18	2

The enhanced shielding properties of the PMMA\_A/AgGF composite materials prepared with the addition of the EMPy-TFSI can be explained by a lubrication effect, induced by the absorption of the ionic liquid onto the surface of the AgGF fillers. This can be indeed confirmed by SEM investigations that indicate a loss of integrity of the Ag coatings for composite samples prepared without the presence of the ionic liquid (Fig. 9). For this analysis, four different types of samples have been investigated: AgGF fillers as received (Fig. 9a,e), AgGF fillers extracted from the composite PMMA\_A/10%AgGF (Fig. 9b,f), AgGF fillers extracted from the composite PMMA\_B / 10%AgGF (Fig. 9c,g) and AgGF fillers extracted from the composite PMMA\_A / 10%AgGF prepared by adding 20 vol% of EMPy-TFSI (Fig. 9d,h). The loss of integrity of the silver coatings for the composite materials PMMA\_A/10%AgGF and PMMA\_B/10%AgGF is clearly evidenced by the missing coating zones on the surface of the microfibers (Fig.9 (f, g)) as well as by detached Ag layers (Fig.9(g)). Obviously, these damage effects are expected to lead to a dramatic decrease in conductivity and shielding properties which is indeed observed in our study. On contrary, these damage effects have not been observed for the AgGF fillers investigated as received and for AgGF fillers extracted from the composite PMMA\_A / 10% AgGF prepared by adding 20 vol% of EMPy-TFSI.

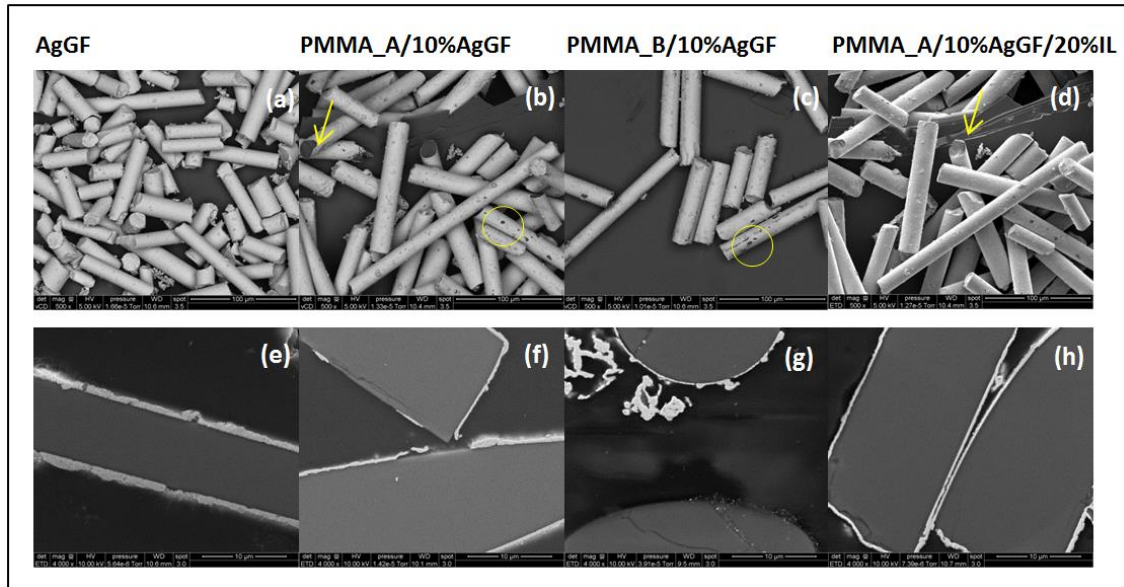


**Figure 9:** images by Scanning Electron Microscopy of: (a, e) AgGF fillers as received. (b, f) AgGF fillers extracted from PMMA\_A/10%AgGF composite material. (c, g) AgGF fillers extracted from PMMA\_B/10%AgGF composite material. (d, h). AgGF fillers extracted from PMMA\_A/10%AgGF/20%IL composite material.

The influence of the ionic liquid can be therefore related to a lubrication effect that helps preserving the integrity of silver coatings during the melt mixing process and allow one thereby to exploit the full potential of these high-performance fillers in developing composite materials with enhanced shielding properties. Two important advantages in using the AgGF fillers can be emphasized. Due to their metallic coating they allow one to obtain a metallic conductivity reaching shielding effectiveness as high as 116 dB. In the same time, due to hybrid nature of the micro-fibers, the fillers have a much lower effective density ( $2.8 \text{ g/cm}^3$ ) than usual metal fillers ( $10.5 \text{ g/cm}^3$  for pure silver). This represents an essential aspect when light composite materials with enhanced electromagnetic shielding are required. The only critical challenge that was to be solved, successfully addressed in the present study by employing an ionic liquid as a functional aid, was the integration without damage of these highly sensitive fillers into the polymer matrix. Several other studies reported in the scientific literature pointed-out the impact of different additives on the shielding properties of composite materials. For instance, Huang et al's [19] studied nickel carbon fibers(NCF)/acrylonitrile butadiene styrene (ABS) composite materials and highlighted that the incorporation of calcium stearate as lubricant enhanced the shielding effectiveness by 38 dB. This result was explained by the fact that calcium stearate is

an additive that facilitates the processing of composites by improving the flow properties and reducing the adhesion of the melt to the machine parts. In addition, calcium stearate is a high-performance dispersion aid, so the addition of lubricants not only prevents fiber breaking by reducing the viscosity of the polymer, but also improves fiber dispersion. Ionic liquids have been also used as lubricants in previous studies [43,44] but not in relation to the electromagnetic shielding properties of composite materials.

#### **4. Conclusions**

The electromagnetic interference shielding effectiveness of poly(methyl-methacrylate) based composite materials filled with silver coated glass microfibers have been investigated by a coaxial cell method in the frequency range from  $10^5$  to  $10^9$  Hz. A substantial decrease in the percolation threshold and an enhancement in the shielding effectiveness by more than 60 dB is found by adding a highly compatible ionic liquid (1-ethyl-4-methylpyridinium bis(trifluoromethylsulfonyl)) into the composite materials. This enhancement effect is due to the interactions between the ionic liquid, the polymer matrix and the filler, leading to a more efficient percolation network. Polymer-based composite materials with shielding effectiveness values up to 116 dB are obtained, as compared to a maximum value of 43 dB reached in the absence of the ionic liquid. The use of ionic liquids can represent thus a very efficient approach to greatly enhance the shielding effectiveness of polymer based composite materials.

#### **5. Acknowledgements**

The financial support of the FUI project NextGen and of the Region Rhône-Alpes is highly acknowledged. The support of the Technological Centre of Microstructures at the University Claude Bernard Lyon (CTμ, Centre Technologique des Microstructures) is highly acknowledged.

## References

- [1] Geetha S, Kumar KKS. EMI shielding: Methods and materials—A review. *J Appl Polym Sci* **2009**, *112*, 2073–2086
- [2] Chung DDL. Materials for electromagnetic interference shielding. *J Mater Eng Perform* **2000**, *9*, 350
- [3] Thomassin J-M, Jérôme C, Pardoën T, Bailly C, Huynen I, Detrembleur C. Polymer/carbon based composites as electromagnetic interference (EMI) shielding materials. *Mater Sci Eng R Rep* **2013**, *74*, 211
- [4] Al-Saleh MH, Saadeh WH, Sundararaj U. EMI shielding effectiveness of carbon based nanostructured polymeric materials: A comparative study. *Carbon* **2013**, *60*, 146
- [5] Hao Wang, Shaonan Li, Mengyue Liu, Jihang Li, Xing Zhou. Review on Shielding Mechanism and Structural Design of Electromagnetic Interference Shielding Composites. *Macromolecular Materials and Engineering* **2021**, *306*, 2100032
- [6] Mondal S, Nayak L, Rahaman M, Aldalbahi A, Chaki TK, Khastgir D, et al. An effective strategy to enhance mechanical, electrical, and electromagnetic shielding effectiveness of chlorinated polyethylene-carbon nanofiber nanocomposites. *Compos Part B Eng* **2017**, *109*, 155
- [7] Sankaran S, Deshmukh K, Ahamed MB, Khadheer Pasha SK. Recent advances in electromagnetic interference shielding properties of metal and carbon filler reinforced flexible polymer composites: A review. *Compos Part Appl Sci Manuf* **2018**, *114*, 49
- [8] Ningmin Duan, Zhenyu Shi, Jilai Wang, Guilong Wang, Xianzhi Zhang. Strong and Flexible Carbon Fiber Fabric Reinforced Thermoplastic Polyurethane Composites for High-Performance EMI Shielding Applications. *Macromolecular Materials and Engineering* **2020**, *305*, 1900829
- [9] Feng Qin, Zhiyang Yan, Jinfeng Fan, Jinliang Cai, Xingzhong Zhu, Xiaogang Zhang. Highly Uniform and Stable Transparent Electromagnetic Interference Shielding Film Based on Silver Nanowire–PEDOT:PSS Composite for High Power Microwave Shielding. *Macromolecular Materials and Engineering* **2020**, *306*, 2000607
- [10] Bauhofer W, Kovacs JZ. A review and analysis of electrical percolation in carbon nanotube polymer composites. *Compos Sci Technol* **2009**, *69*, 1486–1498
- [11] Balberg I, Binenbaum N, Wagner N. Percolation Thresholds in the Three-Dimensional Sticks System. *Phys Rev Lett* **1984**, *52*, 1465–1468

- [12] Jiang Z, Zhang H, Han J, Liu Z, Liu Y, Tang L. Percolation model of reinforcement efficiency for carbon nanotubes dispersed in thermoplastics. *Compos Part Appl Sci Manuf* **2016**, *86*, 49–56
- [13] Paul CR. *Introduction to Electromagnetic Compatibility*. Wiley Son 2006.
- [14] Chung DDL. Electromagnetic interference shielding effectiveness of carbon materials. *Carbon* **2001**, *39*, 279–285
- [15] Ravindren R, Mondal S, Nath K, Das NCh. Investigation of electrical conductivity and electromagnetic interference shielding effectiveness of preferentially distributed conductive filler in highly flexible polymer blends nanocomposites. *Compos Part Appl Sci Manuf* **2019**, *118*, 75–89
- [16] Qin F, Brosseau C. A review and analysis of microwave absorption in polymer composites filled with carbonaceous particles. *J Appl Phys* **2012**, *111*, 061301
- [17] Ghezghapan SMS, Javadi A. Effect of processing methods on electrical percolation and electromagnetic shielding of PC/MWCNTs nanocomposites. *Polymer Composites* **2017**, *38*, E269–276
- [18] Lee SH, Kim JY, Koo CM, Kim WN. Effects of processing methods on the electrical conductivity, electromagnetic parameters, and EMI shielding effectiveness of polypropylene/nickel-coated carbon fiber composites. *Macromol Res* **2017**, *25*, 936–943
- [19] Huang C-Y, Pai J-F. Studies on processing parameters and thermal stability of ENCF/ABS composites for EMI shielding. *J Appl Polym Sci* **1997**, *63*, 115–23
- [20] Thomassin J-M, Pagnoulle C, Bednarz L, Huynen I, Jerome R, Detrembleur C. Foams of polycaprolactone/MWNT nanocomposites for efficient EMI reduction. *J Mater Chem* **2008**, *18*, 792
- [21] Fletcher A, Gupta MC, Dudley KL, Vedeler E. Elastomer foam nanocomposites for electromagnetic dissipation and shielding applications. *Compos Sci Technol* **2010**, *70*, 953–958
- [22] Yan D-X, Ren P-G, Pang H, Fu Q, Yang M-B, Li Z-M. Efficient electromagnetic interference shielding of lightweight graphene/polystyrene composite. *J Mater Chem* **2012**, *22*, 18772
- [23] Ameli A, Jung PU, Park CB. Electrical properties and electromagnetic interference shielding effectiveness of polypropylene/carbon fiber composite foams. *Carbon* **2013**, *60*, 379–391
- [24] Yanjuan Liang, Yelong Tong, Zechao Tao, Quanguo Guo, Baoyi Hao, Zhanjun Liu. Multifunctional Shape-Stabilized Phase Change Materials with Enhanced Thermal

Conductivity and Electromagnetic Interference Shielding Effectiveness for Electronic Devices. *Macromolecular Materials and Engineering* **2021**, *306*, 2100055.

[25] Kar GP, Biswas S, Bose S. Tuning the microwave absorption through engineered nanostructures in co-continuous polymer blends. *Mater Res Express* **2016**, *3*, 064002

[26] Dou R, Shao Y, Li S, Yin B, Yang M. Structuring tri-continuous structure multiphase composites with ultralow conductive percolation threshold and excellent electromagnetic shielding effectiveness using simple melt mixing. *Polymer* **2016**, *83*, 34–9

[27] Revathy Ravindren, Subhadip Mondal, Poushali Bhawal, Shek. Mahammad Nasim Ali, Narayan Chandra Das. Superior electromagnetic interference shielding effectiveness and low percolation threshold through the preferential distribution of carbon black in the highly flexible polymer blend composites. *Polymer Composites* **2018**, *40*, 1404-1418

[28] Arash Sadeghi, Razieh Moeini, Jafar Khademzadeh Yeganeh. Highly conductive PP/PET polymer blends with high electromagnetic interference shielding performances in the presence of thermally reduced graphene nanosheets prepared through melt compounding. *Polymer Composites* **2018**, *40*, E1461-E1469

[29] Zhai W, Zhao S, Wang Y, Zheng G, Dai K, Liu C, et al. Segregated conductive polymer composite with synergistically electrical and mechanical properties. *Compos Part Appl Sci Manuf* **2018**, *105*, 68–77

[30] Soares da Silva JP, Soares BG, Livi S, Barra GMO. Phosphonium–based ionic liquid as dispersing agent for MWCNT in melt-mixing polystyrene blends: Rheology, electrical properties and EMI shielding effectiveness. *Mater Chem Phys* **2017**, *189*, 162–168

[31] Soares BG, Cordeiro E, Maia J, Pereira ECL, Silva AA. The effect of the noncovalent functionalization of CNT by ionic liquid on electrical conductivity and electromagnetic interference shielding effectiveness of semi-biodegradable polypropylene/poly(lactic acid) composites. *Polymer Composites* **2020**, *41*, 82-93

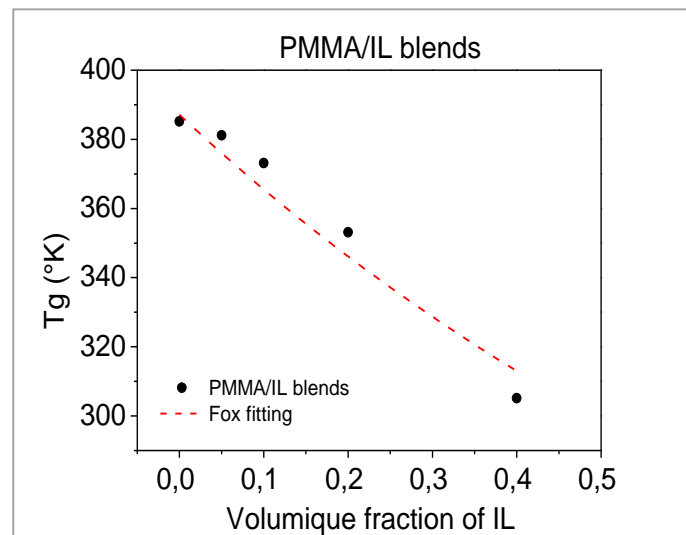
[32] Wu M, Shaw L. Electrical and mechanical behaviors of carbon nanotube-filled polymer blends. *J Appl Polym Sci* **2006**, *99*, 477–88

[33] Cohen MH, Turnbull D. Molecular Transport in Liquids and Glasses. *J Chem Phys* **1959**, *31*, 1164–1169

[34] Zhang L, Wang LB, See KY, Ma J. Effect of carbon nanofiber reinforcement on electromagnetic interference shielding effectiveness of syntactic foam. *J Mater Sci* **2013**, *48*, 7757–7763

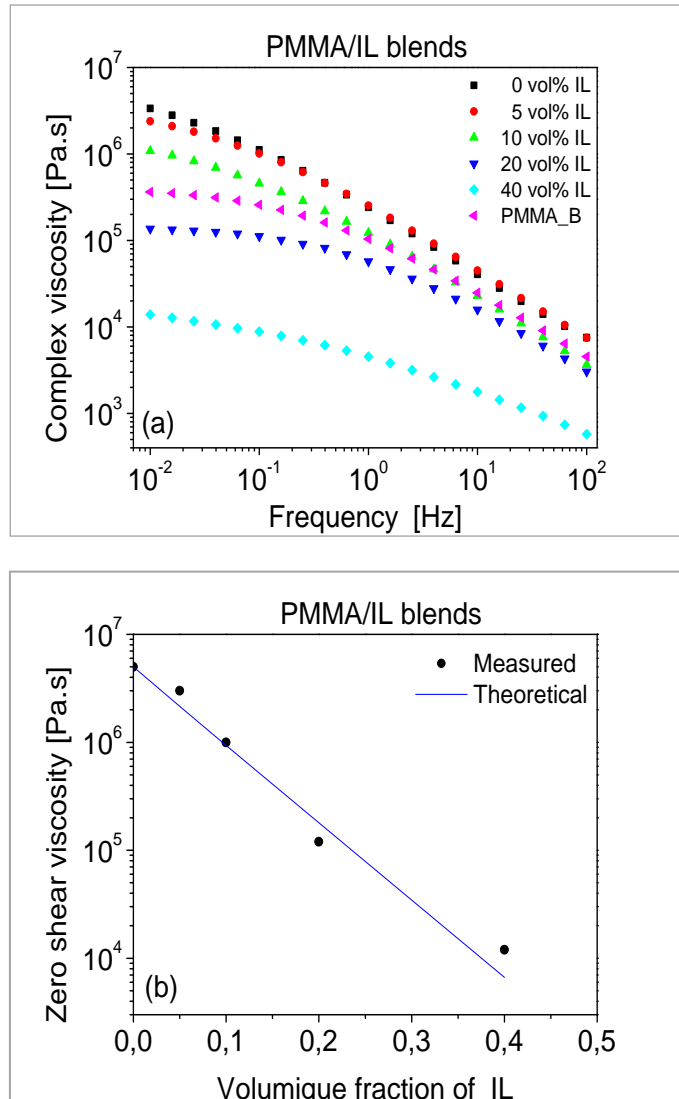
- [35] Rohini R, Bose S. Electromagnetic Interference Shielding Materials Derived from Gelation of Multiwall Carbon Nanotubes in Polystyrene/Poly(methyl methacrylate) Blends. *ACS Appl Mater Interfaces* **2014**, *6*, 11302–11310
- [36] Ameli A, Nofar M, Wang S, Park CB. Lightweight Polypropylene/Stainless-Steel Fiber Composite Foams with Low Percolation for Efficient Electromagnetic Interference Shielding. *ACS Appl Mater Interfaces* **2014**, *6*, 11091–100
- [37] Wu H, Wang C, Ma C, Chiu Y, Chiang M, Chiang C. Preparations and properties of maleic acid and maleic anhydride functionalized multiwall carbon nanotube/poly(urea urethane) nanocomposites. *Compos Sci Technol* **2007**, *67*, 1854–60
- [38] Thomassin J-M, Huynen I, Jerome R, Detrembleur C. Functionalized polypropylenes as efficient dispersing agents for carbon nanotubes in a polypropylene matrix; application to electromagnetic interference (EMI) absorber materials. *Polymer* **2010**, *51*, 115–121
- [39] Im JS, Park IJ, In SJ, Kim T, Lee Y-S. Fluorination effects of MWCNT additives for EMI shielding efficiency by developed conductive network in epoxy complex. *J Fluor Chem* **2009**, *130*, 1111–1116
- [40] Sung-Hoon Park, Theilmann PT, Asbeck PM, Bandaru PR. Enhanced Electromagnetic Interference Shielding Through the Use of Functionalized Carbon-Nanotube-Reactive Polymer Composites. *IEEE Trans Nanotechnol* **2010**, *9*, 464–469
- [41] Mohammed H. Al-Saleh, Uttandaraman Sundararaj. Electromagnetic Interference (EMI) Shielding Effectiveness of PP/PS Polymer Blends Containing High Structure Carbon Black. *Macromolecular Materials and Engineering* **2008**, *293*, 621-630.
- [42] Soares BG, Touchaleaume F, Calheiros LF, Barra GMO. Effect of double percolation on the electrical properties and electromagnetic interference shielding effectiveness of carbon-black-loaded polystyrene/ethylene vinyl acetate copolymer blends. *J Appl Polym Sci* **2016**, *133*, 43013
- [43] Sanes J, Carrión FJ, Bermúdez MD, Martínez-Nicolás G. Ionic liquids as lubricants of polystyrene and polyamide 6-steel contacts. Preparation and properties of new polymer-ionic liquid dispersions. *Tribol Lett* **2006**, *21*, 121–133
- [44] Kamimura H, Kubo T, Minami I, Mori S. Effect and mechanism of additives for ionic liquids as new lubricants. *Tribol Int* **2007**, *40*, 620–625

## Supplementary Information



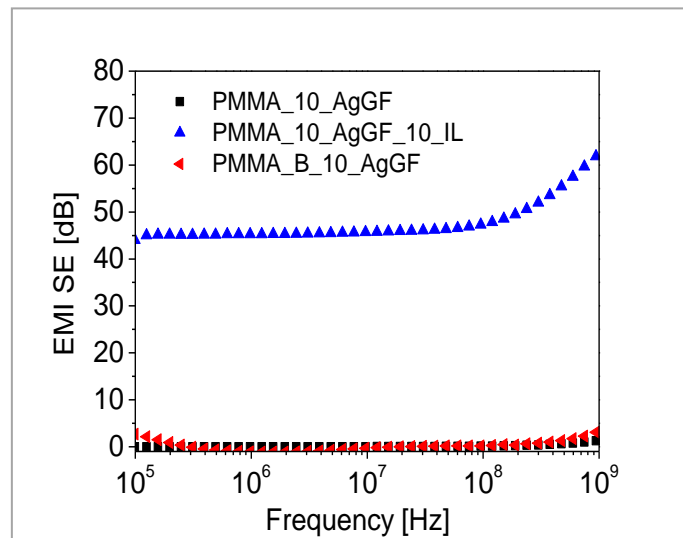
**Figure S1:** The glass transition temperature  $T_g$  of PMMA/EMPy-TFSI blends as a function of the IL concentration, measured by Differential Scanning Calorimetry.

## Supplementary Information



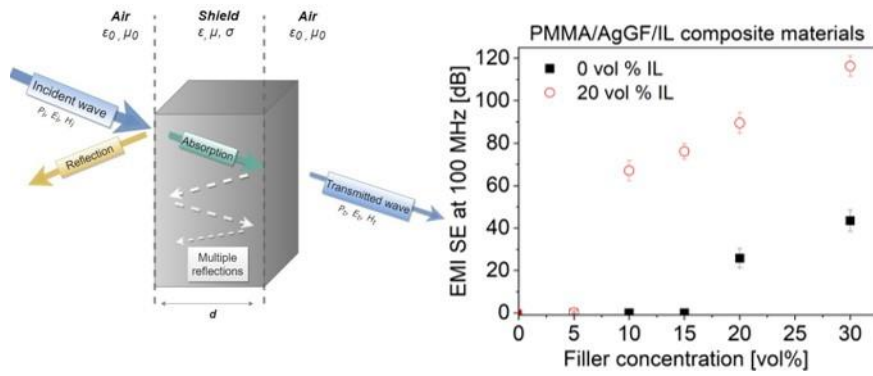
**Figure S2:** (a) complex viscosity of PMMA / EMPy-TFSI blends as a function of frequency, at different concentrations of the ionic liquid. Additionally, the data on PMMA\_B are shown. (b) the zero shier viscosity of PMMA / EMPy-TFSI blends as a function of the IL concentration. The line represents the theoretical fit.

## Supplementary Information



**Figure S3:** Electromagnetic interference shielding effectiveness of PMMA\_A/10vol%\_AgGF composite material, of PMMA\_B/10vol% AgGF composite material and of PMMA\_A/10vol% AgGF composite material prepared by adding 10 vol% of the ionic liquid EMPy-TFSI.

## Table of contents



The addition of an ionic liquid leads to a substantial enhancement, by more than 60 dB, of the interference shielding effectiveness of PMMA based composite materials filled with silver-coated microfibers. This is explained by the interaction between the ionic liquid, the polymer matrix and the silver coated microfibers that lead to a more efficient percolation network.